ACS Energy LETTERS

http://pubs.acs.org/journal/aelccp

Quantification of Lithium Battery Fires in Internal Short Circuit

Shanhai Ge, Tatsuro Sasaki, Nitesh Gupta, Kaiqiang Qin, Ryan S. Longchamps, Koichiro Aotani, Yuichi Aihara, and Chao-Yang Wang*

Cite This: *ACS Energy Lett.* 2024, 9, 5747−5755

Read Online

ACCESS | Metrics & More | Article Recommendations | Supporting Information

ABSTRACT: Single-layer internal shorting in a multilayer battery is widely considered among the "worst-case" failure scenarios leading to thermal runaway and fires. We report a highly reproducible method to quantify the onset of fire/smoke during internal short circuiting (ISC) of lithium-ion batteries (LiBs) and anode-free batteries. We unveil that lithium metal batteries (LMBs) with or without liquid electrolytes are more dangerous than LiBs upon internal shorting, igniting fires within a time scale of 1−3 s followed by similar or larger combustion heat release. This implies that all solid state batteries (ASSBs) with lithium anodes will have safety concerns, and much research is needed to scrutinize ASSB safety. Also, there exists a threshold in the shorting current to trigger a fire in LMBs, and its precise control is key to reproducing ISC behaviors. Finally, we unravel the profound role of oxygen in fire/smoke formation and present new suggestions for developing safe ASSBs.

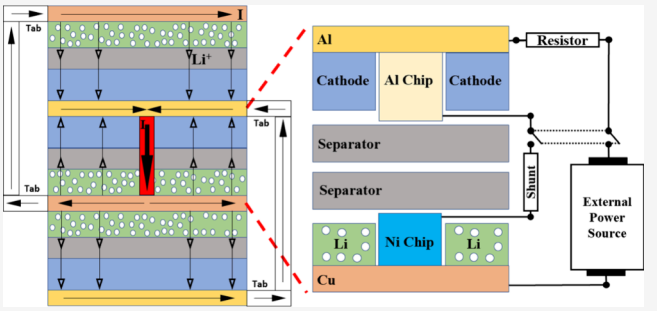

The safety of lithium-ion and lithium metal batteries is a critical barrier for electric vehicles to go mainstream for transportation decarbonization.[1−4] Thermal runaway (TR) and fires caused by internally shorting battery cells have been examined through several abuse tests such as nail penetration,[5−7] embedding low-melting point materials,[8] patch heaters,[9] crush, external short circuit,[10] and calorimetry,[11] in accordance with many standards and regulations developed by International Electrotechnical Commission (IEC), the International Organization for Standardization (ISO), and the Society of Automotive Engineers International (SAE).[12] Unfortunately, quantitative and reproducible experimental studies of battery fires are still absent, which makes it difficult to probe the fundamental science of lithium battery fires and impossible to quantitatively compare the effects of dominant factors and, hence, the effectiveness of mitigation strategies.[13] However, general discussions of battery safety abound in the literature, e.g. refs 10, 14, and 15.

The occurrence of single-layer internal shorting in a multilayer battery is widely considered to be among the "worst-case" failure scenarios.[16] As illustrated in Figure 1a, all energy from the neighboring intact layers is discharged through the small spot of the ISC layer, thus generating a huge amount of heat locally. Combustion ensues if there is a combination of heat input, fuel, and oxidizer. Complete combustion is observed as a fire, whereas incomplete combustion resulting from insufficient oxidizer manifests as smoke. Here, we report a new experimental method to quantitatively study the onset of fire or smoke during single-layer internal shorting of lithium-ion batteries (LiBs) and anode-free batteries (AFBs). We show that lithium metal AFBs with and without liquid electrolytes are more dangerous than LiBs upon internal shorting, generating fires within a time scale of 1−3 s. This implies that all solid-state batteries with a lithium metal anode are not immune from safety concerns. Also, there exists a threshold in the shorting current or heating power to trigger a fire. Finally, we reveal a profound effect of oxygen by employing layered oxide cathodes charged at various states of charge (SOC) as well as contrasting with a lithium iron phosphate (LFP) cathode.

Figure 1a (left) schematically depicts the physical problem of single-layer internal shorting in a multilayer battery, and Figure 1a (right) displays an experimental apparatus designed to replicate it. A single-layer cell is developed with two thin metal chips embedded to induce internal shorting (Figure

Received: September 16, 2024
Revised: October 11, 2024
Accepted: October 30, 2024
Published: November 6, 2024

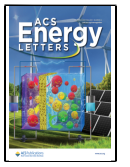

https://doi.org/10.1021/acsenergylett.4c02564
ACS Energy Lett. 2024, 9, 5747−5755

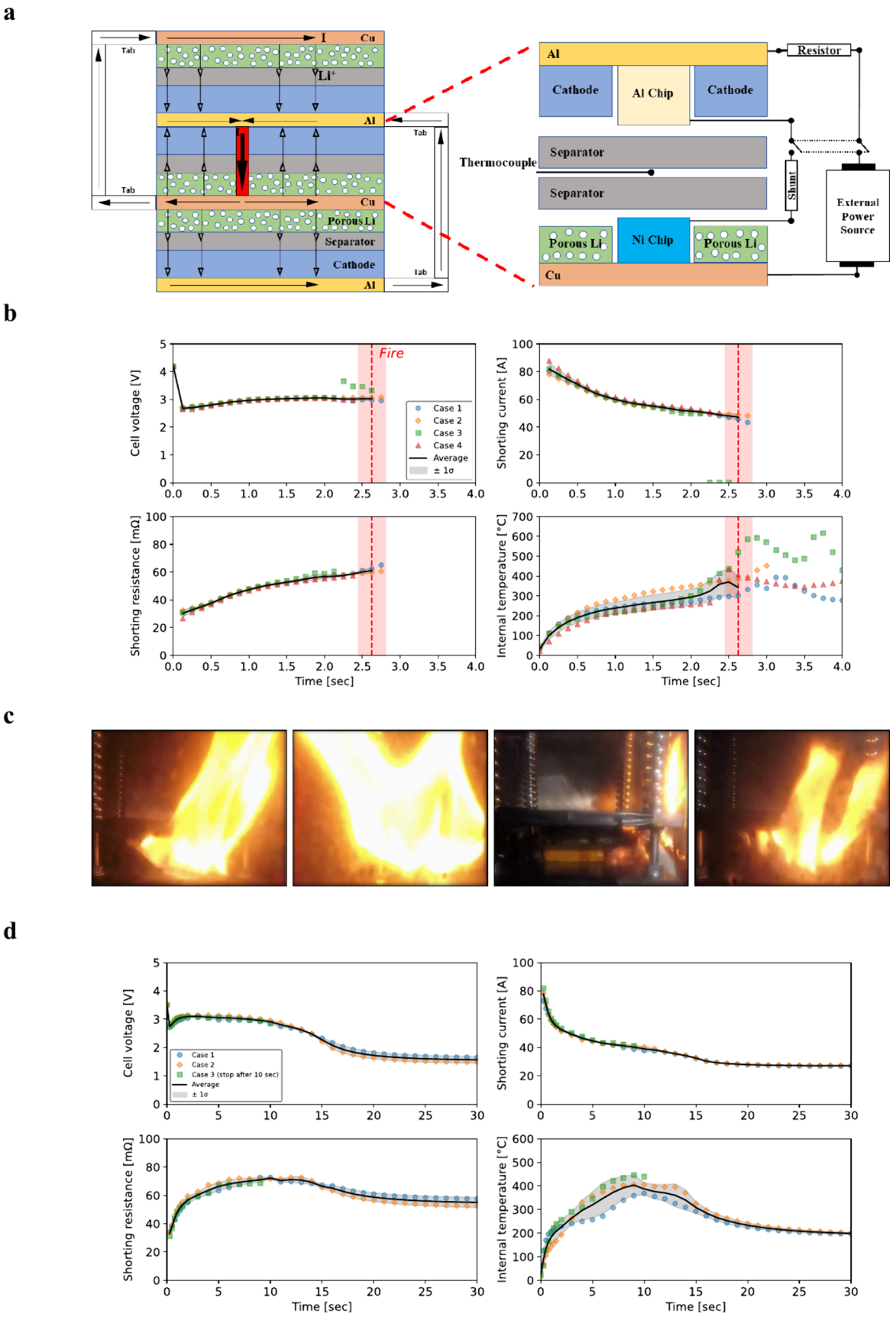

Figure 1. Single-layer internal shorting of lithium metal batteries. a, Illustration of the physical problem and corresponding experimental setup. b, Reproducibility tests of an anode-free cell with NMC 811 cathode where shaded areas represent errors of $\pm 1\ \sigma$. All four cells catch fire around 2.6 s (marked by the vertical dashed line) after the start of internal shorting. c, Photos of the four cells in b at $t = 3.6$ s after ISC. d, Reproducibility tests of anode-free cells with LFP cathode where shaded areas represent errors of $\pm 1\ \sigma$. There is no fire in all three cells.

https://doi.org/10.1021/acsenergylett.4c02564
ACS Energy Lett. 2024, 9, 5747−5755

Table 1. Heat of Combustion of Fuels per cm^2 of Electrode in Various Batteries

fuel sources	thickness (m)	heat of combustion (J/kg)	mass (kg/cm^2)	heat (J/cm^2)
In LiBs				
ethylene carbonate (30 wt %)		1.214×10^{07}[17]	1.697×10^{-06}	20.60
ethyl methyl carbonate (70 wt %)		1.841×10^{07}[18]	3.959×10^{-06}	72.89
total				**93.49**
In AFBs				
20 μm Li metal deposited at 100% SOC	2.000×10^{-05}	4.300×10^{07}[19]	1.068×10^{-06}	45.92
DME in electrolyte		3.169×10^{07}[20]	1.116×10^{-06}	35.37
TTE in electrolyte		1.051×10^{07}[21]	7.186×10^{-06}	75.52
total (AFB with LHCE)				**156.81**
total (solvent-free AFB)				**45.92**
In ASSBs w/20 μm Li Foil				
20 μm Li foil + 20 μm deposited at 100% SOC	4.000×10^{-05}	4.300×10^{07}[19]	2.136×10^{-06}	91.85
total				**91.85**

S1a). An aluminum chip is placed against the cathode current collector by removing the porous cathode coating for direct contact. A nickel chip is pressed against the anode current collector in an anode-free configuration. The two chips are connected externally by a switch and a shunt resistor. When the switch is on, the single-layer cell is internally shorted with the shorting current measured over the shunt. Neighboring unshorted layers are lumped together and represented by an external power source of a 2.6 Ah battery, which is then connected in parallel with the single-layer cell to be shorted. An extra resistor is added to the circuit to systematically adjust the shorting current and, hence, heating power. Other details of the experimental apparatus, cell materials, instrumentation, and test procedures can be found in the Methods section of the Supporting Information. All videos related to the experiments reported in this paper can also be found therein.

Reproducibility and accuracy of the new measurement system were first verified for a set of four single-layer AFB cells of 0.15 Ah with $LiNi_{0.8}Mn_{0.1}Co_{0.1}O_2$ (NMC811) cathode under identical conditions. As shown in Figure 1b, the measured variations of cell voltage, shorting current, and shorting resistance are found to be within 5%, whereas that of internal temperature is within 20% since the local temperature is most difficult to reproduce due to steep spatial gradients. Moreover, all four cases catch fire, marked by the vertical dashed line in Figure 1b, at 2.6 s with variations of ±0.18 s, which is less than 10%. Large scattering of internal temperature after the onset of fire is ignored in data analysis because once the violent fires breaks out, the test cells get disintegrated and lose their structural integrity with the thermocouple. Figure 1c displays images of Cases 1−4 at 3.6 s, shortly after fire ignition. Similarly, reproducibility tests were performed for a set of 3 AFBs with a lithium iron phosphate (LFP) cathode under identical conditions. Figure 1d again shows that the measurement variations of cell voltage, shorting current, and shorting resistance are within 5%, whereas internal temperature is within 20%. Notably, there was no fire in all three LFP cases due to the absence of oxygen. The high degree of reproducibility displayed in Figure 1b− d is satisfactory for performing parametric experiments in order to quantitatively identify dominant factors for battery fires.

EFFECT OF FUELS

Fuel sources for battery fires include carbonate electrolytes in conventional LiBs, lithium metal and liquid solvents/diluents in AFBs with localized high-concentration electrolytes (LHCE), and lithium metal only in solvent-free AFB cells. The latter is developed as a mockup for all solid state batteries (ASSBs) with lithium metal anodes. Table 1 lists the heat of combustion of the above fuels. Clearly, the heating values of fuels in the four types of batteries, LiBs, AFBs with solvents/diluents, solvent-free AFBs, and all solid ASSBs, are comparable. Notably, ASSBs merely replace flammable electrolyte in LiBs with more reactive lithium metal as the fuel with comparable heat release from combustion (91.85 vs 93.69 J/cm^2). The mock solid cell, a solvent-free AFB with only 45.92 J/cm^2 combustion heat, represents the lower bound in combustion energy of ASSB cells.

Figure 2a compares the internal shorting of an AFB with LHCE to a LiB (see Table S1 for their cell design specifications), both having the same NMC811 cathode. From a combustion point of view, the two cells differ in fuel sources, with the AFB having a heating value of 156.81 J/cm^2 and the presence of highly reactive lithium metal versus the LiB having 93.69 J/cm^2 and without lithium metal. It is clearly seen that the internal shorting of the AFB cell is much more violent, catching fire at 2.6 s, whereas the LiB only ejects smoke around 4 s (Figure 2b). Both cells have similar shorting resistance and current, indicating similar heating power during ISC. The internal temperature in the AFB rises to ∼400 °C, where a fire is already triggered due to the high reactivity of molten lithium. In contrast, the internal temperature in the LiB can rise to 800 °C before smoke formation, implying that complete combustion of carbonate electrolytes with oxygen released from the NMC cathode is more difficult to occur. Indeed, the theoretical amount of oxygen needed for complete combustion of carbonate solvents largely exceeds that releasable from the NMC cathode.

Figure 2c compares ISC experiments of the AFB with LHCE to another identical AFB cell but with liquid solvents/diluents evaporated under vacuum overnight. Such a solvent-free AFB reduces the fuel source's heating value from 156.81 to 45.92 J/cm^2, with the latter attributed only to lithium metal. All other properties remain virtually the same; for example, the cell voltage and shorting resistance are the same between the two cells, as shown in Figure 2c. The total shorting current is slightly lower in the solvent-free AFB layer as that layer without electrolyte does not produce ionic current during short circuiting. The solvent-free AFB is seen to catch fire at 1.6 s, even earlier than 2.6 s of the AFB with liquid LHCE. This can be explained by the more facile transport of oxygen gas released from the NMC cathode into the lithium metal anode

https://doi.org/10.1021/acsenergylett.4c02564
ACS Energy Lett. 2024, 9, 5747−5755

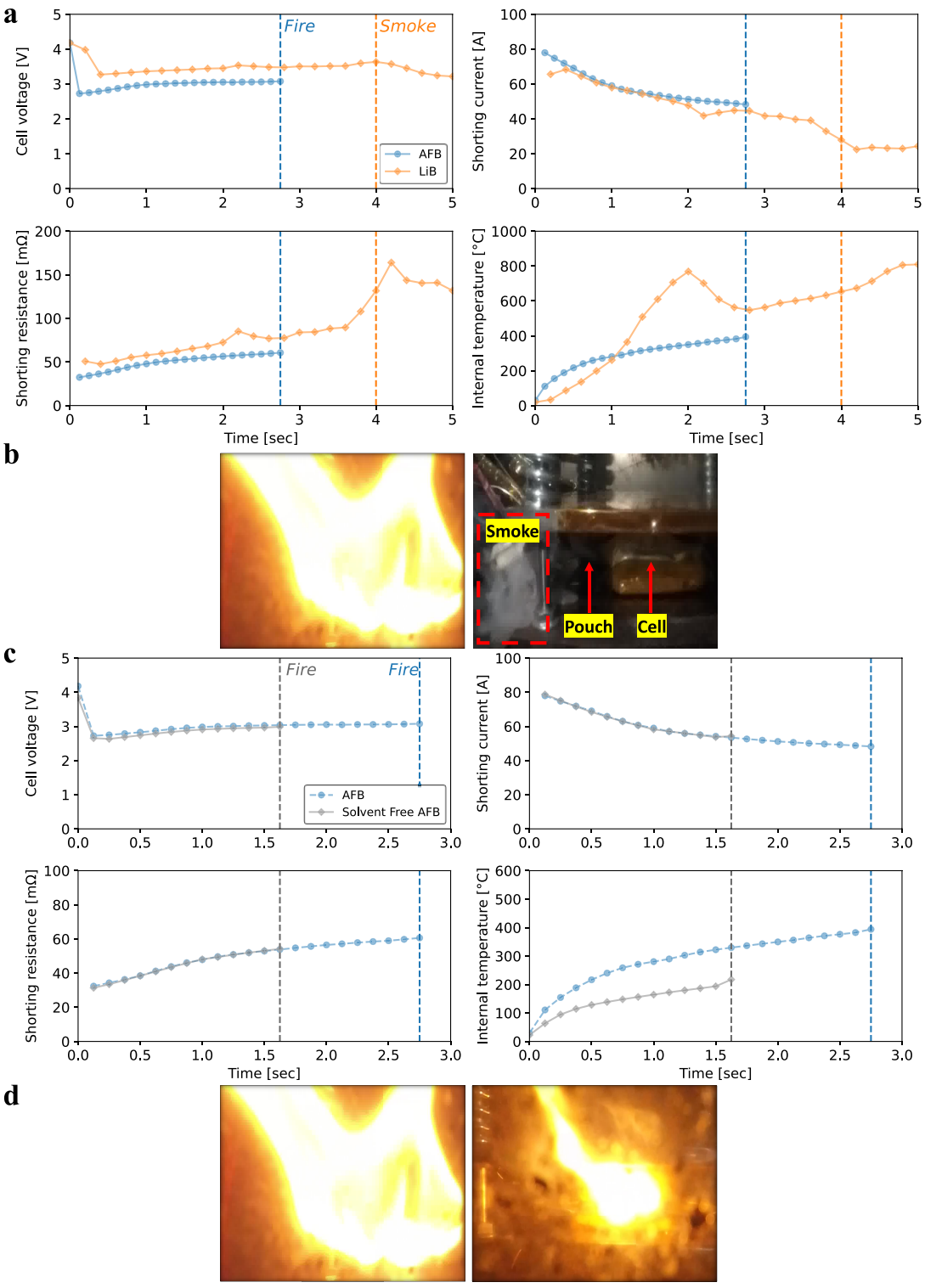

Figure 2. Effect of fuels on lithium battery safety. a, AFB with LHCE vs LiB. b, Photos of AFB at 3.60 s and LiB at 4.75 s. c, AFB cells with and without liquid solvents. d, photos of the AFB at 3.6 s and solvent-free AFB at 2.25 s. See the heating values of fuels in various types of batteries in Table 1.

through open pores of a dry separator without liquid electrolyte. It can also be noted from Figure 2c that at the onset of fire, the solvent-free AFB has an internal temperature rising to only ~200 °C, whereas the normal AFB with liquid LHCE rises to ~400 °C. This difference in ignition temperature may be related to lithium metal in contact with gaseous O_2 in the solvent-free AFB or O_2 dissolved in the liquid electrolyte in the baseline AFB. Figure 2d displays fire images of AFB and solvent-free AFB. Both fires are violent, with the one in the AFB lasting much longer than in the solvent-free AFB, consistent with almost 3.5× heating release from the AFB versus the solvent-free AFB, as calculated in Table 1.

https://doi.org/10.1021/acsenergylett.4c02564
ACS Energy Lett. 2024, 9, 5747−5755

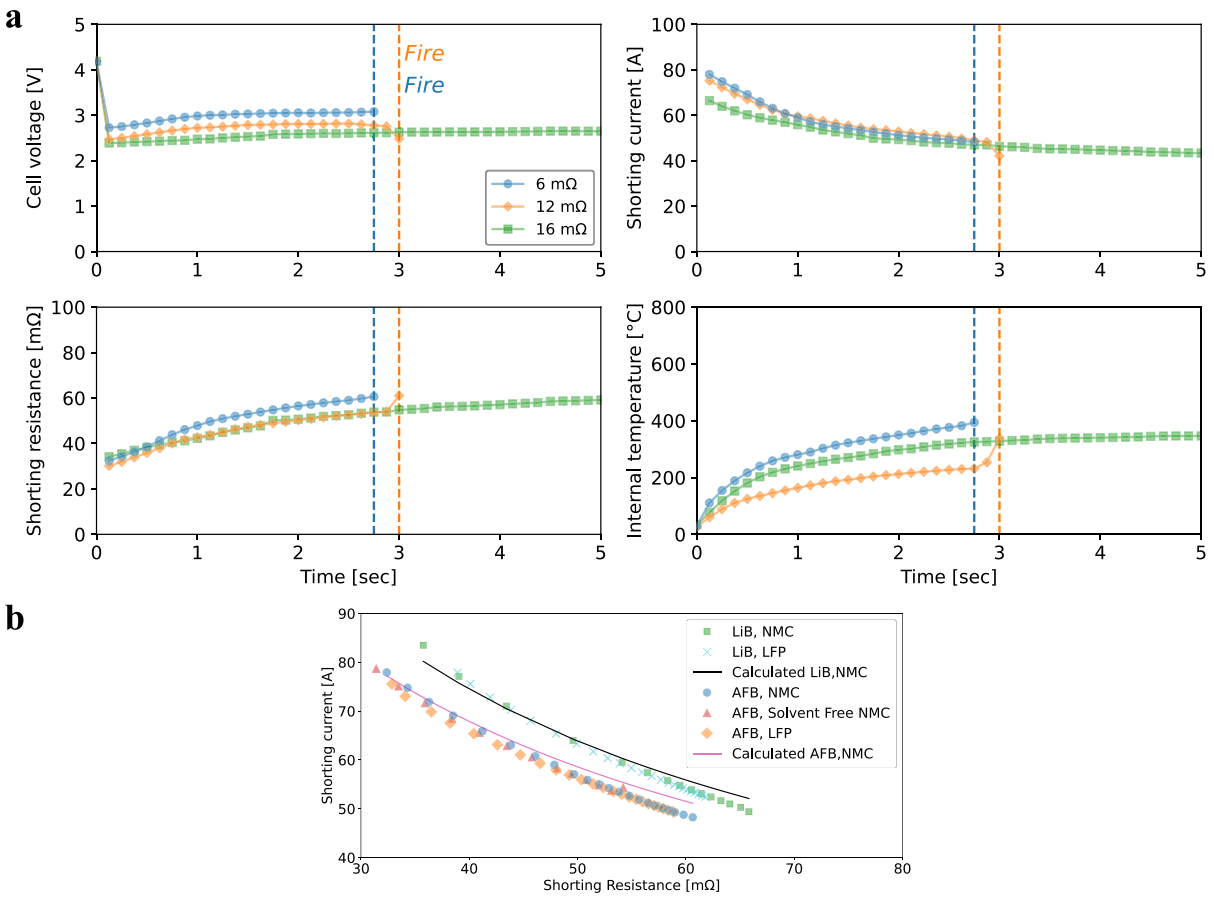

Figure 3. Effect of shorting current, as varied by adding extra resistors. a, cell voltage, shorting current, shorting resistance, and internal temperature after single-layer ISC. b, Shorting current is controlled primarily by shorting resistance in various AFB cells and LiB cells, respectively.

EFFECT OF SHORTING CURRENT (AND HEATING POWER)

Another critical factor that triggers battery combustion is heat input, which is proportional to the square of the shorting current. We systematically vary the shorting current by adding extra resistors in our measurement loop, as displayed in Figure 1a (right). Figure 3a shows three experiments of the AFB with the extra resistor of 6, 12, and 16 mΩ, respectively. It is seen that the initial shorting current drops from 81 to 67 A correspondingly. Both 6 and 12 mΩ cases, having the initial shorting current of 81 and 78 A, catch fires at 2.4 and 3.0 s upon short circuiting, respectively. However, when the initial shorting current drops to 67 A in the case of 16 mΩ, there is no fire. This demonstrates that there exists a threshold of shorting current (and hence heating power), around ∼70A, to trigger battery fires. Converted into C-rate, this threshold is equivalent to ∼27C of the 2.6Ah battery. Note also that the internal temperature plot in Figure 3a shows a clear bump at the onset of fire for both 6 and 12 mΩ cases. Figure 3b displays relationships between the shorting current and shorting resistance for two groups of batteries, AFBs and LiBs. Within the AFB group, although the experimental data are obtained from cells with different cathodes (NMC vs LFP) and electrolytes (LHCE vs solvent-free), they all merge into a single relationship between the shorting current and shorting resistance. The same goes for the LiB group. Such a trend could be explained by an equivalent circuit diagram of the ISC experimental setup, as depicted in Figure S9. Indeed, Figure 3b shows that the predicted results (solid lines) are in good agreement with the experimental data.

The existence of a threshold shorting current to trigger fire suggests that there may be neither fire nor smoke in cases of soft shorting where the shorting resistance is sufficiently high and the shorting current is low. Thus, it is of paramount importance to control the shorting resistance precisely in quantitative studies of ISC consequences. The importance of shorting resistance may also explain the seemingly stochastic nature of ISC behaviors in the field and prior laboratory studies that have failed to report and precisely control this key experimental parameter. A technological implication of the threshold shorting current discovered here is that lithium metal batteries may avoid fires by designing and engineering cells with larger internal resistance, e.g. by employing polymer−metal composite current collectors.

EFFECT OF OXIDIZER

Oxygen is needed for lithium metal combustion, and hence, battery fires commonly originate from layered oxide cathodes. To confirm this hypothesis, two AFBs, one with the NMC811 cathode as the baseline and the other with the LFP cathode, are internally shorted. Figure 4a clearly shows that the NMC-based AFB catches fire, whereas the LFP-based AFB has neither fire nor smoke. Despite the two cells having a disparity in open circuit voltage, the cell voltage becomes quickly similar once short circuiting, and the shorting resistance and current are similar. The internal temperature in the NMC-based AFB

https://doi.org/10.1021/acsenergylett.4c02564
ACS Energy Lett. 2024, 9, 5747−5755

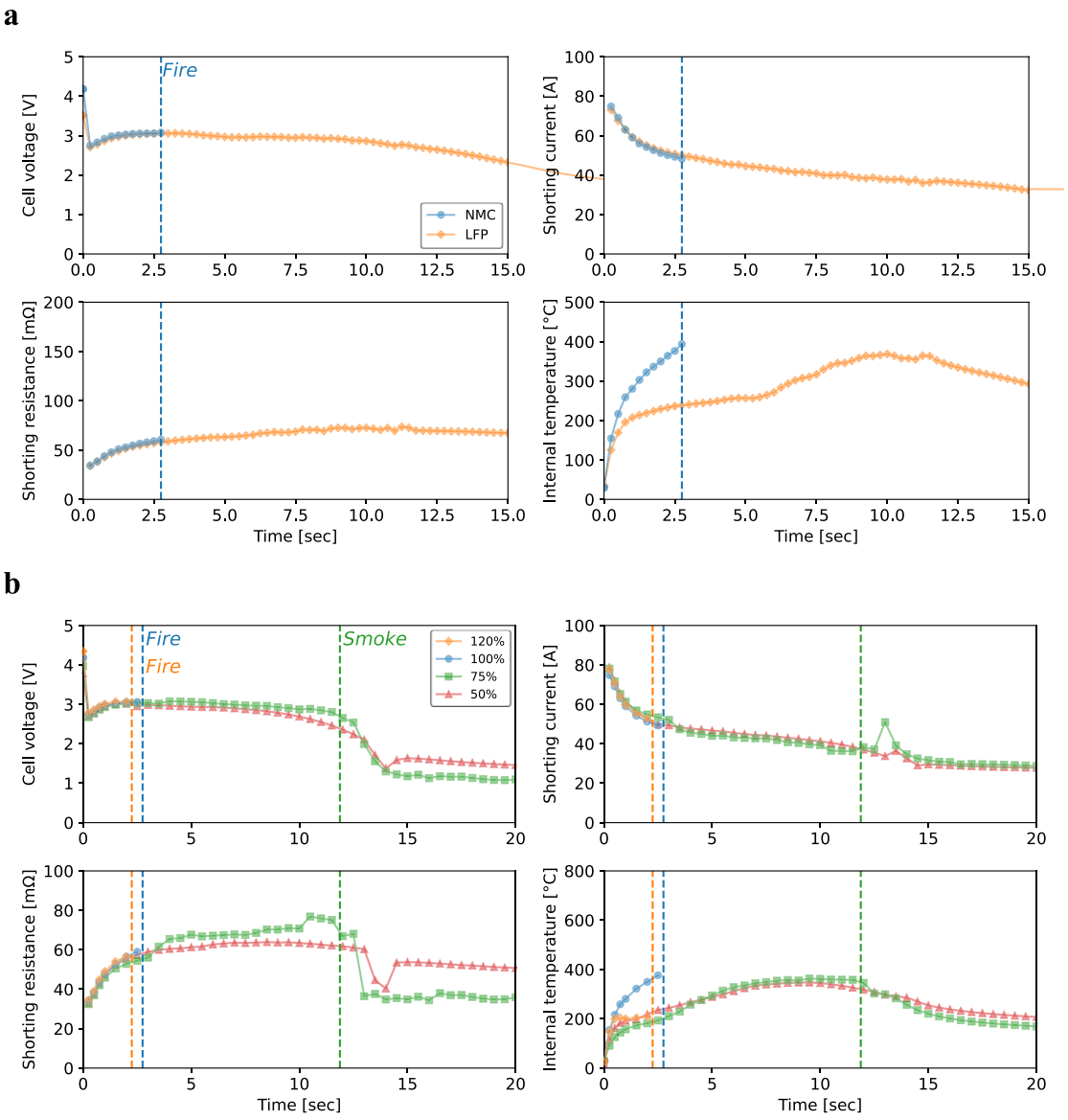

Figure 4. Effect of oxidizer on lithium battery safety after single-layer ISC. a, NMC vs LFP cathode. b, NMC cathodes charged to varying states of charge (SOC).

rises to ~400 °C shortly after the start of fire, whereas that in the LFP-based AFB also rises to a similar level but fails to ignite fire or smoke. Figure 4b further compares four AFBs with the NMC cathode charged to various states of charge (SOC). The higher the SOC, the more oxygen is released upon heating during short circuiting. Both 120% and 100% SOC cases catch fire around the same time (~2.6 s) upon internal shorting, whereas the 75% SOC case has a delayed smoke formation around 12 s, and the 50% SOC case incurs neither fire nor smoke. The results in Figure 4 demonstrate the profound importance of oxidizer in fire formation, pointing out that the separation of O_2 from lithium metal should be an important direction to suppress or eliminate fire/smoke for lithium metal battery safety.

Based on the fundamental theory of combustion, we have elucidated lithium battery fires by considering heat input, fuel, and oxidizer. Using a newly developed experimental method for single-layer internal shorting, quantitatively reproducible results have been obtained to study a range of parameters affecting fire/smoke formation and, hence, battery safety under the "worst-case" scenario. It is found that all batteries containing lithium metal have sufficient conditions to catch fires in a time scale of 1−3 s, irrespective of liquid electrolytes. Such a short time scale of the fire onset makes pack-level safety measures virtually impossible, and we must seek viable solutions inside battery cells, including chemistry, materials and internal structure. Otherwise, lithium metal batteries are intrinsically unsafe, both in terms of the kinetic potency to catch fire and the large heat release thereafter.

There exists a threshold of shorting current and, hence, heating power to trigger a fire in lithium metal batteries. Thus, it is crucial to control and quantify the shorting resistance in reproducible studies of ISC behaviors. Hard or soft internal shorting in the field, characterized by disparate orders of magnitude in shorting resistance, will lead to vastly different ISC consequences that have appeared statistical in nature. Deterministic predictions from ISC computer modeling shall identify the shorting resistance as the key input parameter and give the shorting current as the key output in order to properly characterize ISC behaviors. Also, intentionally increasing the

https://doi.org/10.1021/acsenergylett.4c02564
ACS Energy Lett. 2024, 9, 5747−5755

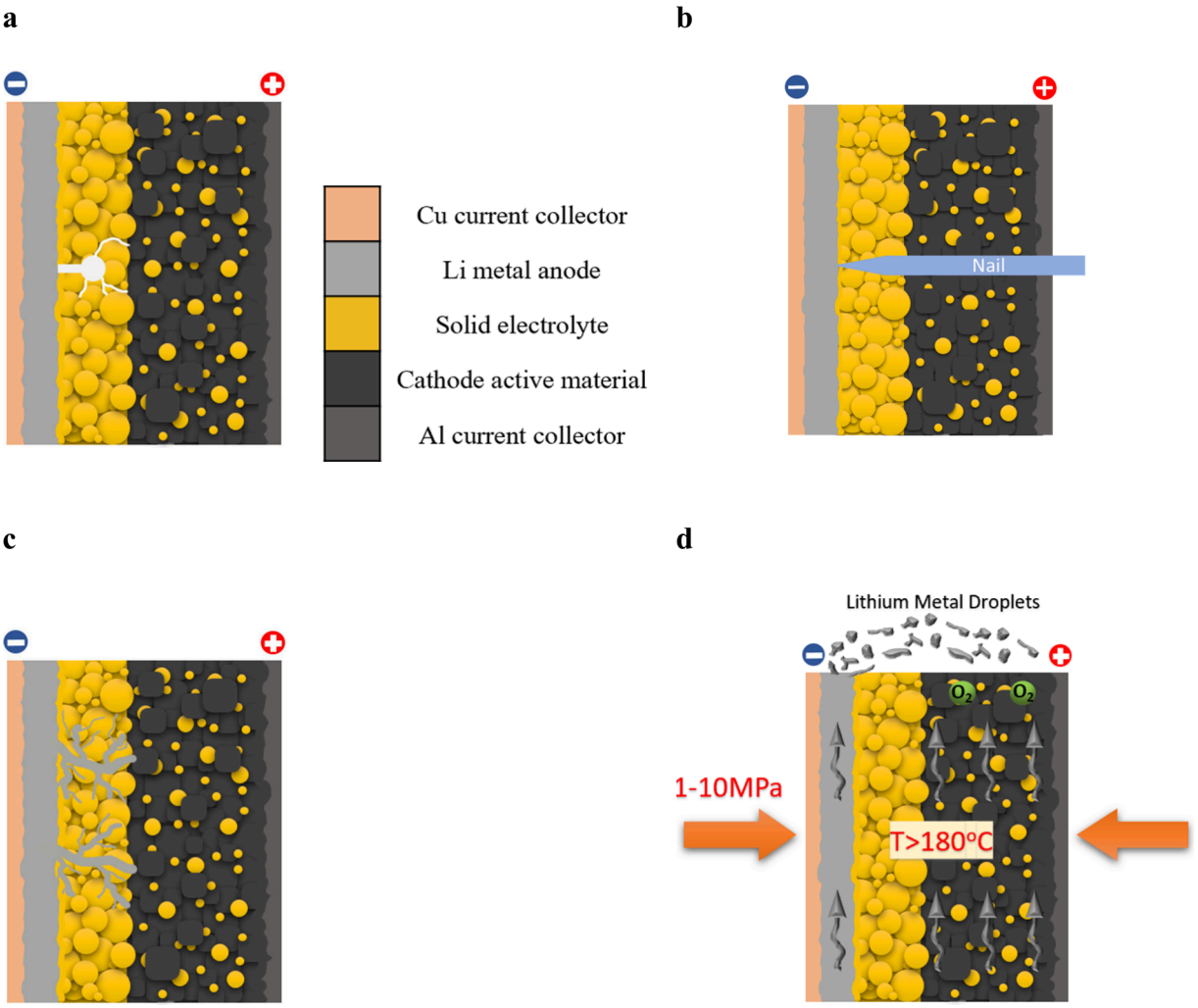

Figure 5. Sketches of lithium metal coming in contact with oxygen in ASSBs under hypothetical abuse conditions. a, O_2 diffusion through pores, cracks and defects of solid separator. b, O_2 permeated into anode in nail penetration. c, Lithium dendrites grows into O_2-evolving cathode. d, Molten lithium droplets squeezed or oozed out by cell clamping pressure.

internal resistance of lithium metal batteries, including ASSBs, and hence decreasing the shorting current may prove effective in avoiding fires and realizing safety, but such a measure will curb ASSBs' ambition to achieve fast charge and high-power discharge. Additionally, shorting current control by use of positive-temperature-coefficient (PTC) materials may be effective. Oxygen released from layered oxide cathodes and its transport into the lithium metal anode plays a major role in fire/smoke formation; as such, fire/smoke suppression seemingly lies in ways to block or isolate oxygen released in cathodes from direct contact with lithium metal.

Finally, the results presented herein clearly show that ASSBs with lithium metal anodes are bound to catch fire or even explode so long as lithium metal has access to oxygen evolving from a cathode. There are multiple pathways for fire formation in ASSBs with lithium metal. The most generic one prevailing is molten lithium combustion:[22]

$$4Li + O_2 \rightarrow 2Li_2O \quad \Delta H = 4.3 \times 10^7\ J/kg$$

This reaction requires a theoretical oxygen-fuel (OF) molar ratio of 0.25, whereas a delithiated NMC cathode can release 0.5 OF oxygen theoretically. Thus, there is sufficient oxygen supply in NMC-based ASSBs. Other pathways may involve: (a) exothermic reactions between solid electrolytes, such as argyrodite type LPSCl, and delithiated NMC cathodes triggering fires at 150 °C and subsequent thermal runaway;[23] and (b) highly exothermic reactions between molten lithium and oxygen released from inorganic solid electrolytes such as $Li_{1.5}Al_{0.5}Ge_{1.5}(PO_4)_3$ (LAGP) and $Li_{1.4}Al_{0.4}Ti_{1.6}(PO_4)_3$ (LATP).[24] The present work only addresses the above-mentioned most generic pathway, which is irrespective of electrolyte, and hence, our mock solid cell without an electrolyte is appropriate.

There are numerous abuse conditions under which oxygen released from cathode active materials may come in contact with lithium metal on the anode side, as schematically illustrated in Figure 5. Examples are that (a) oxygen from the cathode diffuses through open pores, cracks and defects of <100% dense solid electrolyte separators placed between the anode and cathode (Figure 5a), (b) the solid separator is pierced during nail penetration or broken by mechanical impact (Figure 5b), (c) lithium dendrites grow through inorganic solid separators (e.g., along grain boundaries) to reach the cathode (Figure 5c), and (d) molten lithium metal at 180 °C and above is squeezed out of the cell edge by ultrahigh stack pressure of a few MPa to arrive at the oxygen-releasing

https://doi.org/10.1021/acsenergylett.4c02564
ACS Energy Lett. 2024, 9, 5747−5755

cathode (Figure 5d). An example of the scenario depicted in Figure 5a is the connected cracks formed across a ceramic separator, as discovered by the Bruce group[25] in ASSBs. The ISC result of the solvent-free cell presented in this study is thus directly relevant to this type of ASSBs.

It can be seen from Figure 2 that all batteries containing lithium metal, including ASSBs, have sufficient conditions to catch fire in a short time scale of 1 to 3 s. Although the thermodynamic prediction of unsafe ASSBs with lithium metal anode was made by Longchamps et al.[15] and later independently by Bates et al.[26] in the prior literature, the present study provides such experimental evidence for the first time. The short time scale of triggering fires in lithium metal batteries, including ASSBs, is a grave concern as it makes pack-level safety measures virtually in vain. Therefore, addressing the safety issue should be among the highest R&D priorities for ASSBs, if not the most important one.

■ ASSOCIATED CONTENT

Supporting Information

The Supporting Information is available free of charge at https://pubs.acs.org/doi/10.1021/acsenergylett.4c02564.

Experimental methods, performance and cycle life of AFB single-layer cells, equivalent circuit analysis of ISC process, and morphological and compositional characterization of anodes after ISC, and additional figures, a table, and references (PDF)

First reproducibility test video of single layer shorting of an anode free cell with NMC811 cathode (MP4)

Second reproducibility test video of single layer shorting of an anode free cell with NMC811 cathode (MP4)

Third reproducibility test video of single layer shorting of an anode free cell with NMC811 cathode(MP4)

First reproducibility test video of single layer shorting of an anode free cell with LFP cathode (MP4)

Second reproducibility test video of single layer shorting of an anode free cell with LFP cathode (MP4)

Third reproducibility test video of single layer shorting of an anode free cell with LFP cathode (MP4)

Lithium-ion battery with an NMC811 cathode and graphite anode single layer shorting (MP4)

Solvent free anode free battery with an NMC811 cathode single layer shorting (MP4)

Single layer shorting of an anode free battery with an NMC811 cathode and 6 mΩ resistance (MP4)

Single layer shorting of an anode free battery with an NMC811 cathode and 12 mΩ resistance (MP4)

Single layer shorting of an anode free battery with an NMC811 cathode and 16 mΩ resistance (MP4)

Single layer shorting of an anode free battery with an NMC811 cathode charged to 120% SOC (MP4)

Single layer shorting of an anode free battery with an NMC811 cathode charged to 100% SOC (MP4)

Single layer shorting of an anode free battery with an NMC811 cathode charged to 75% SOC (MP4)

Single layer shorting of an anode-free battery with an NMC811 cathode charged to 50% SOC (MP4)

■ AUTHOR INFORMATION

Corresponding Author

Chao-Yang Wang − *Electrochemical Engine Center (ECEC) and Department of Mechanical Engineering, The Pennsylvania State University, University Park, Pennsylvania 16802, United States;* orcid.org/0000-0003-0650-0025; Email: cxw31@psu.edu

Authors

Shanhai Ge − *Electrochemical Engine Center (ECEC) and Department of Mechanical Engineering, The Pennsylvania State University, University Park, Pennsylvania 16802, United States;* orcid.org/0000-0003-2882-1276

Tatsuro Sasaki − *Nissan Research Center, Nissan Motor Co. Ltd., Yokosuka, Kanagawa 237-8523, Japan*

Nitesh Gupta − *Electrochemical Engine Center (ECEC) and Department of Mechanical Engineering, The Pennsylvania State University, University Park, Pennsylvania 16802, United States*

Kaiqiang Qin − *Electrochemical Engine Center (ECEC) and Department of Mechanical Engineering, The Pennsylvania State University, University Park, Pennsylvania 16802, United States*

Ryan S. Longchamps − *Electrochemical Engine Center (ECEC) and Department of Mechanical Engineering, The Pennsylvania State University, University Park, Pennsylvania 16802, United States;* orcid.org/0000-0002-8168-8032

Koichiro Aotani − *Nissan Research Center, Nissan Motor Co. Ltd., Yokosuka, Kanagawa 237-8523, Japan*

Yuichi Aihara − *Nissan Research Center, Nissan Motor Co. Ltd., Yokosuka, Kanagawa 237-8523, Japan*

Complete contact information is available at: https://pubs.acs.org/10.1021/acsenergylett.4c02564

Author Contributions

S.G. and T.S. contributed equally to this paper.

Notes

The authors declare no competing financial interest.

■ ACKNOWLEDGMENTS

Financial support from Nissan Motor Co. Ltd. is gratefully acknowledged.

■ REFERENCES

(1) Whittingham, M. S. Lithium batteries and cathode materials. *Chem. Rev.* **2004**, *104*, 4271−4301.

(2) Lu, B.; Cheng, D.; Sreenarayanan, B.; Li, W.; Bhamwala, B.; Bao, W.; Meng, Y. S. Key Parameters in Determining the Reactivity of Lithium Metal Battery. *ACS Energy Lett.* **2023**, *8*, 3230−3238.

(3) Zheng, S.; Wang, L.; Feng, X.; He, X. Probing the heat sources during thermal runaway process by thermal analysis of different battery chemistries. *J. Power Sources* **2018**, *378*, 527−536.

(4) Liu, K.; Liu, Y.; Lin, D.; Pei, A.; Cui, Y. Materials for Lithium-Ion Battery Safety. *Sci. Adv.* **2018**, *4*, No. eaas9820.

(5) Finegan, D. P.; Tjaden, B.; Heenan, T. M.; Jervis, R.; Di Michiel, M.; Rack, A.; Hinds, G.; Brett, D. J.; Shearing, P. R. Tracking Internal Temperature and Structural Dynamics during Nail Penetration of Lithium-Ion Cells. *J. Electrochem. Soc.* **2017**, *164*, A3285−A3291.

(6) Lamb, J.; Orendorff, C. J. Evaluation of mechanical abuse techniques in lithium ion batteries. *J. Power Sources.* **2014**, *247*, 189−196.

(7) Liu, S.; Huang, S.; Zhou, Q.; Snyder, K.; Long, M. K.; Zhang, G. In Situ Measurement of Dynamic Internal Short Circuit Resistance during Nail Penetration of Lithium-Ion Cells and its Implications on Cell Robustness and Abuse Tolerance. *J. Electrochem. Soc.* **2023**, *170*, No. 060515.

(8) Finegan, D. P.; et al. Characterising thermal runaway within lithium-ion cells by inducing and monitoring internal short circuits. *Energy Environ. Sci.* **2017**, *10*, 1377−1388.

(9) Lopez, C. F.; Jeevarajan, J. A.; Mukherjee, P. P. Experimental Analysis of Thermal Runaway and Propagation in Lithium-Ion Battery Modules. *J. Electrochem. Soc.* **2015**, *162*, A1905−A1915.
(10) Doughty, D.; Roth, E. P. A General Discussion of Li Ion Battery Safety. *Electrochem Soc. Interface* **2012**, *21*, 37−44.
(11) Inoue, T.; Mukai, K. Are all-solid-state lithium-ion batteries really safe?−verification by differential scanning calorimetry with an all-inclusive microcell. *ACS Appl. Mater. Interfaces* **2017**, *9*, 1507−1515.
(12) Ruiz, V.; Pfrang, A.; Kriston, A.; Omar, N.; Van den Bossche, P.; Boon-Brett, L. A review of international abuse testing standards and regulations for lithium ion batteries in electric and hybrid electric vehicles. *Renewable and Sustainable Energy Reviews* **2018**, *81*, 1427−1452.
(13) Walker, W. Q.; Darst, J. J.; Finegan, D. P.; Bayles, G. A.; Johnson, K. L.; Darcy, E. C.; Rickman, S. L. Decoupling of heat generated from ejected and non-ejected contents of 18650-format lithium-ion cells using statistical methods. *J. Power Sources* **2019**, *415*, 207−218.
(14) Feng, X.; Ren, D.; He, X.; Ouyang, M. Mitigating Thermal Runaway of Lithium-Ion Batteries. *Joule* **2020**, *4*, 743−770.
(15) Longchamps, R. S.; Yang, X. G.; Wang, C. Y. Fundamental Insights into Battery Thermal Management and Safety. *ACS Energy Lett.* **2022**, *7*, 1103−1111.
(16) Zhao, W.; Luo, G.; Wang, C. Y. Modeling Internal Shorting Process in Large-Format Li-ion Cells. *J. Electrochem. Soc.* **2015**, *162*, A1352−A1364.
(17) Choi, J. K.; Joncich, M. J. Heats of Combustion, Heats of Formation and Vapor Pressures of Some Organic Carbonates Estimation of Carbonate Group Contribution to Heat of Formation. *J. Chem. Eng. Data* **1971**, *16*, 87−90.
(18) Eshetu, G. G.; Grugeon, S.; Laruelle, S.; Boyanov, S.; Lecocq, A.; Bertrand, J. P.; Marlair, G. In-depth safety-focused analysis of solvents used in electrolytes for large scale lithium ion batteries. *Phys. Chem. Chem. Phys.* **2013**, *15*, 9145−9155.
(19) Heat of Combustion of the elements. https://periodictable.com/Properties/A/CombustionHeat.al.html. Accessed on October 11, 2024.
(20) Pilcher, G.; Pell, A. S.; Coleman, D. J. Measurements of Heats of Combustion by Flame Calorimetry Part 2.-Dimethyl Ether, Methyl Ethyl Ether, Methyl n-Propyl Ether, Methyl IsoPropyl Ether. *Trans. Faraday Soc.* **1964**, *60*, 499−505.
(21) Van Duin, A. C. T., ReaxFF Calculations of TTE combustion reactions, *private communication*, May 2024.
(22) Inoue, T.; Mukai, K. Are All-Solid-State Lithium-Ion Batteries Really Safe?−Verification by Differential Scanning Calorimetry with an All-Inclusive Microcell. *ACS Appl. Mater.* **2017**, *9*, 1507−1515.
(23) Kim, T.; Kim, K.; Lee, S.; Song, G.; Jung, M. S.; Lee, K. T. Thermal Runaway Behavior of Li_6PS_5Cl Solid Electrolytes for $LiNi_{0.8}Co_{0.1}Mn_{0.1}O_2$ and $LiFePO_4$ in All-Solid-State Batteries. *Chem. Mater.* **2022**, *34*, 9159−9171.
(24) Chen, R.; Nolan, A. M.; Lu, J.; Wang, J.; Yu, X.; Mo, Y.; Chen, L.; Huang, X.; Li, H. The Thermal Stability of Lithium Solid Electrolytes with Metallic Lithium. *Joule* **2020**, *4*, 812−821.
(25) Ning, Z.; Li, G.; Melvin, D. L. R.; Chen, Y.; Bu, J.; Spencer-Jolly, D.; Liu, J.; Hu, B.; Gao, X.; Perera, J.; Gong, C.; Pu, S. D.; Zhang, S.; Liu, B.; Hartley, G. O.; Bodey, A. J.; Todd, R. I.; Grant, P. S.; Armstrong, D. E. J.; Marrow, T. J.; Monroe, C. W.; Bruce, P. G. Dendrite initiation and propagation in lithium metal solid-state batteries. *Nature* **2023**, *618*, 287−293.
(26) Bates, A. M.; Preger, Y.; Torres-Castro, L.; Harrison, K. L.; Harris, S. J.; Hewson, J. Are solid-state batteries safer than lithium-ion batteries? *Joule* **2022**, *6*, 742−755.

https://doi.org/10.1021/acsenergylett.4c02564
ACS Energy Lett. 2024, 9, 5747−5755